

Thermal Response of Tritiated Codeposits from JET and TFTR to Transient Heat Pulses

This article has been downloaded from IOPscience. Please scroll down to see the full text article.

2003 Phys. Scr. 2003 34

(<http://iopscience.iop.org/1402-4896/2003/T103/006>)

View [the table of contents for this issue](#), or go to the [journal homepage](#) for more

Download details:

IP Address: 192.12.184.6

The article was downloaded on 15/05/2012 at 15:05

Please note that [terms and conditions apply](#).

Thermal Response of Tritiated Codeposits from JET and TFTR to Transient Heat Pulses

C. H. Skinner^{1,*}, N. Bekris², J. P. Coad³, C. A. Gentile¹, A. Hassanein⁴, R. Reiswig⁵ and S. Willms⁵

¹Princeton Plasma Physics Laboratory, Princeton, NJ, USA

²Tritium Laboratory, Forschungszentrum Karlsruhe, Germany

³UKAEA Fusion, Culham Research Centre, Abingdon, Oxon, UK

⁴Argonne National Laboratory, Argonne, Illinois, USA

⁵Los Alamos National Laboratory, Los Alamos, NM 87545, USA

Received May 22, 2002; accepted August 22, 2002

PACS ref: 44.10.+i, 52.90.+z

Abstract

High heat flux interactions with plasma facing components have been studied at microscopic scales. The beam from a continuous wave neodymium laser was scanned at high speed over the surface of graphite and carbon fiber composite tiles that had been retrieved from TFTR and JET after DT plasma operations. The tiles have a surface layer of amorphous hydrogenated carbon that was codeposited during plasma operations and laser scanning has released more than 80% of the codeposited tritium. The temperature rise of the codeposit was much higher than that of the manufactured material and showed an extended time history. The peak temperature varied dramatically (e.g. 1436°C compared to >2300°C) indicating strong variations in the thermal conductivity to the substrate. A digital microscope imaged the codeposit before, during and after the interaction with the laser and revealed 100-micron scale hot spots during the interaction. The heat flux produced a pattern of beads on a mixed Be/C deposit. Heat pulse durations of order 100 ms resulted in brittle destruction and material loss from the surface, whilst a duration of ≈ 10 ms showed minimal changes to the codeposit. These results show that reliable predictions for the response of deposition areas to off-normal events such as ELMs and disruptions in next step devices need to be based on experiments with tokamak generated codeposits.

1. Introduction

The intense heat loads during ELMs and disruptions on plasma facing components in a next step device is a major concern for their survivability and operational lifetime [1–3]. Very high heat flux will produce sublimation, heating and explosion of gases trapped in pores, and thermal stresses and fatigue in graphite and carbon-fiber-composite (CFC) materials. These conditions cannot be duplicated in existing tokamaks because of the large difference in energy stored in the plasma. Even measuring the power deposition during ELMs in existing machines is challenging. Uncertainties in the thermal conductivity of deposited surface layers can lead to factor 3 overestimates of the power flux [4]. Carbon based materials have shown high erosion losses in disruption simulation facilities that use electron beams [5], pulsed lasers [6,7], plasma guns [8], and other high power devices [9]. Comprehensive modeling codes [10] have been used to simulate the conditions from the transport of the core plasma to the scrape-off-layer, the subsequent generation of a vapor shield at the divertor, and the reduced divertor plate lifetime due to melt layer loss and brittle destruction [11].

A scanning laser beam has been used to rapidly heat codeposited layers on tiles from tokamaks and release hydrogen isotopes. Up to 87% of the codeposited tritium

has been thermally desorbed from tile samples from the Joint European Torus (JET) and the Tokamak Fusion Test Reactor (TFTR) in laboratory experiments reported in Refs. [12,13]. The technique is attractive for tritium removal in a next-step DT device since it avoids the use of oxidation, the associated deconditioning of the plasma facing surfaces, and expense of processing large quantities of tritium oxide [14,15]. Although designed for tritium removal, this approach offers an opportunity to study in microscopic detail the thermomechanical response of tokamak generated codeposits to transient high heat fluxes. The response is measured without the complications of vapor shielding, which may attenuate the thermal flux in a tokamak. Laboratory experiments on codeposits on JET and TFTR tiles showed that the temperature rise of the codeposit was significantly higher than that of the manufactured tile material at the same heat flux (e.g. 1770°C cf. 1080°C) indicating a much lower effective thermal conductivity for the codeposits [17]. In the present paper we focus on the thermal response to the laser heat flux and the morphology of the codeposits. The tritium release aspects are reported in Refs. [12,13].

2. Experimental setup

The experimental set up is shown in Fig. 1 and fully described in [12]. Briefly, a 325 W continuous wave Nd laser beam is steered by two orthogonal mirrors and focused inside a chamber containing a tile sample from either JET or TFTR. The laser spot can be scanned over a field of 75 × 75 mm with a velocity of up to 2 m/s. The spot trajectory is defined by programming the motion of the scan mirrors via a computer interface. Typically, a serpentine raster pattern with line spacing 0.5 mm is used to cover the tile surface. The complete laser spot extends over a few mm so a given location on the tile experiences first the fringe of the laser spot, then the center, then the fringe in ≈ 6 successive passes. A pyrometer measures surface temperatures in the range of 500–2300°C with 0.3 ms time resolution and averages over a fixed 0.7 mm area on the tile surface. Before and after laser irradiation the tile surface is photographed by a digital microscope to record any changes in the surface. The atmosphere in the tile chamber was either argon or air. Released tritium was circulated in a closed loop to an ion chamber that measured the tritium concentration. Results from TFTR

*Corresponding author. e-mail: cskinner@pppl.gov

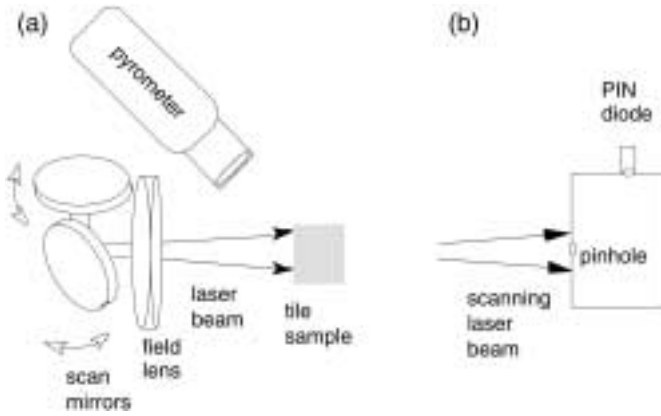


Fig. 1. Experimental Setup.

tiles showed that a major fraction of the tritium was desorbed with minimal changes to the tile surface at a laser intensity of 80 W/mm^2 and scan speeds of the order of 1 m/s [12].

The time dependence of the heat flux from the scanning laser spot was measured by placing a 35-micron pinhole at the same position as used for the tile surface and recording the transmitted laser light with a PIN diode (Fig. 1(b)). The laser system has been recently upgraded with fiber optic coupling between the laser and scanner to mimic the arrangement proposed for the tokamak applications and the focal spot was measured in this configuration. The intensity profile was reconstructed from the laser intensity transmitted through the pinhole during a typical raster scan at full power and speed 1 m/s . The full width half maximum diameter was 1.6 mm similar to previous measurements of marks made by a stationary laser spot on a tile for both fiber coupled and direct coupled cases. With fiber coupling, the maximum laser intensity on the sample was 128 W/mm^2 . At a 1 m/s scan speed and FWHM duration of 1.6 ms the energy deposited is 0.2 MJ/m^2 , about a factor 5 lower than that the maximum acceptable for ITER ELMs [16].

3. Thermal response

The laser beam generated a brilliant incandescent spot, heating the codeposits to temperatures from 1500°C to above 2300°C (the pyrometer operates in the region $500\text{--}2300^\circ\text{C}$). In contrast, the temperature rise for erosion areas or for the original manufactured material was much lower (1000°C to 1500°C). Analytical modeling of a semi-infinite homogeneous solid under a constant heat flux indicated that the results for the codeposit could be matched by arbitrarily reducing both the effective thermal conductivity and density by a factor-of-two compared to the coefficients for the manufactured materials [17]. However it is clear that the deposits are far from being homogeneous.

Figure 2 shows the time history of the temperature excursion of three samples and the laser flux as transmitted by the 35-micron pinhole at the same scan speed in a separate experiment. The laser heating pulse duration is 4 ms , scan speed 1 m/s , laser intensity 80 W/mm^2 and the samples are in argon. The JET sample 1BN4-8-4L reaches a peak temperature of 1434°C and remains above 500°C for 5.3 ms . This sample is from an erosion area on the base

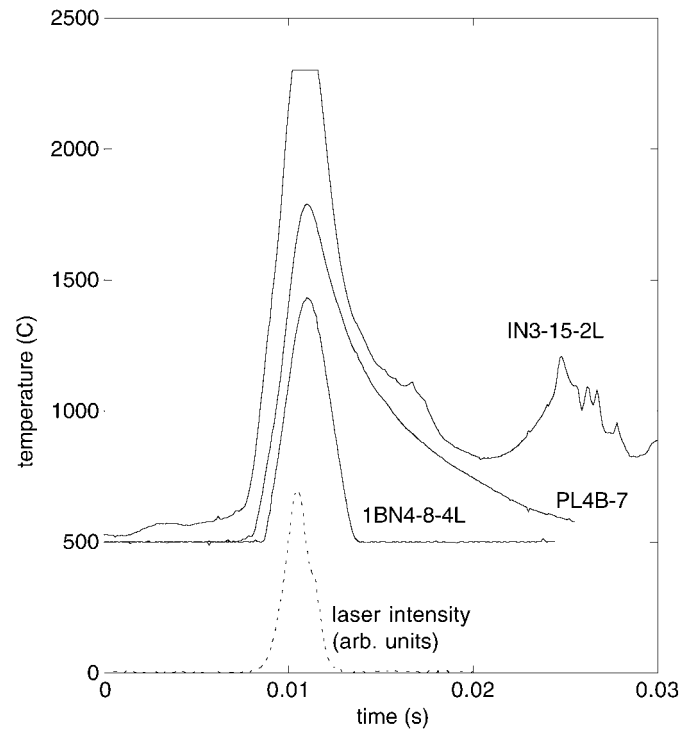


Fig. 2. Temperature response of erosion (1BN4-8-4L) and deposition areas (PL4B7top, IN3-15-2L) to the same local laser intensity of 80 W/mm^2 (measured separately and shown dotted). The pyrometer operates in the region $500\text{--}2300^\circ\text{C}$.

divertor tile 4 on JET. Sample PL4B7top is from a deposition area on the JET poloidal limiter and the temperature response peaks at 1790°C and shows a longer cool down time or “tail” in the time history due to lower conductivity or poor thermal contact between the deposit and underlying tile. JET sample IN3-15-2L had a particularly striking temperature response. This sample is from the lower edge of divertor tile 3 (adjacent to the louvers) and the codeposit had the heaviest tritium concentration of any analyzed JET or TFTR tile. Remarkably, the temperature increases to above 2300°C and then rises again after the laser pulse has passed (before the next pass of the laser spot). This “ragged” character in the temperature time history was evident on several samples with thick codeposits. Even though the ambient atmosphere is argon, XPS analysis [18] has shown atomic concentrations of oxygen of up to 50% (excluding H-isotopes) on these samples from the long exposure to humid air after retrieval from the vessel. These oxides can participate in chemical reactions and oxidation reactions are believed to account for the second temperature peak in the IN3-15-2L trace in Fig. 2.

Non-linear behavior was seen in the variation of temperature with duration of heating. For an idealized homogeneous material, the temperature rise would increase with the square root of the heat pulse duration. In contrast, the peak temperature of TFTR samples did not increase much above 2000°C even when the scan speed was decreased from 1000 mm/s to 25 mm/s [12].

4. Microscopy of the deposits

A low power digital microscope imaged the surface of the tile samples before, during, and after the laser scan. The

original codeposited surface exhibited granulation and irregularities. At high scan speeds (≈ 1 m/s) the relatively short duration of the heating pulse and shallow (≈ 100 micron) depth of the heat penetration [12] resulted in a darkening of the surface but the codeposit appeared largely undisturbed (Fig. 3(b) and Ref. [12]). In contrast, surface damage (Fig. 3(c)) became increasingly evident at slower scan speeds as the incident energy approached 1 MJ/m^2 , underlining the erosion lifetime concern associated with ELMs [16].

Macroscopic erosion of carbon based materials depends on the net power flux to the surface, exposure time and the threshold energy required for brittle destruction. The latter is estimated from disruption simulation experiments using manufactured tile surfaces to be $\approx 10 \text{ kJ/g}$, or 20 kJ/cm^3 [9]. The present experiments indicate that this threshold is significantly lower for codeposits because of their poor thermal contact with the underlying tile. This may be inconsequential for the erosion lifetime of the underlying plasma facing components but will cause impurity influx as the surface layers sublime at high temperatures.

The microscope was used in video mode at 30 frames/s to image the tile surface *during* the laser interaction. A still from the video is shown in Fig. 4. Micro “hotspots” of 100-micron scale are evident within the laser spot indicating that the temperature recorded within the 0.7 mm diameter

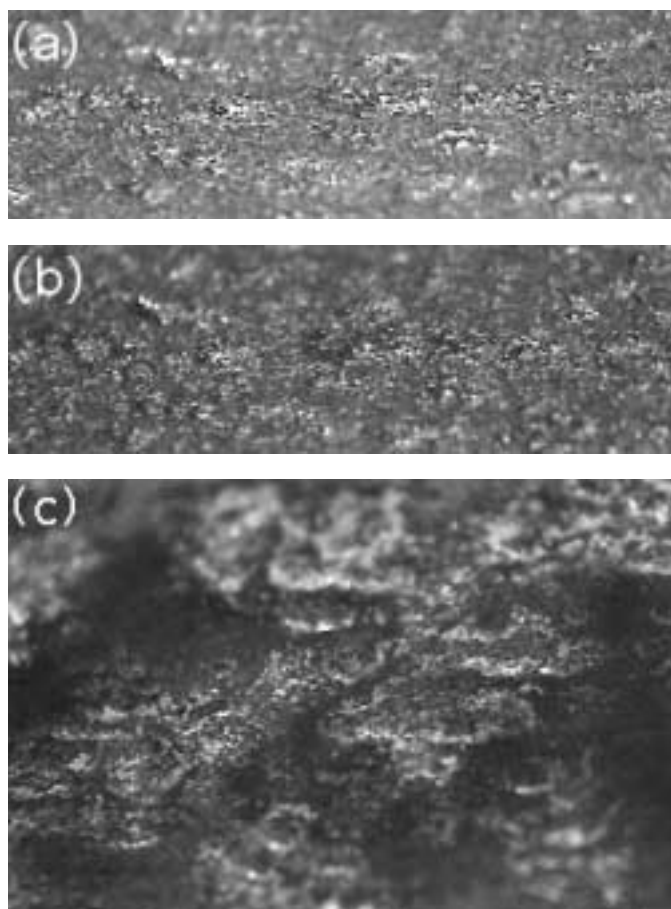


Fig. 3. Low power microscope images of codeposit taken at 45 degrees of TFTR sample KC22-6E before (a) and after (b) a laser scan at 1 m/s and 80 W/mm^2 resulting in a 10 ms temperature excursion above 500°C that peaked at 1770°C releasing of 18 mCi of tritium; (c) TFTR sample KC17-3C after laser scan at 25 mm/s at 80 W/mm^2 . The temperature excursion above 500°C lasted 222ms and peaked at 1925°C . The images cover 7.2 mm in the horizontal direction.

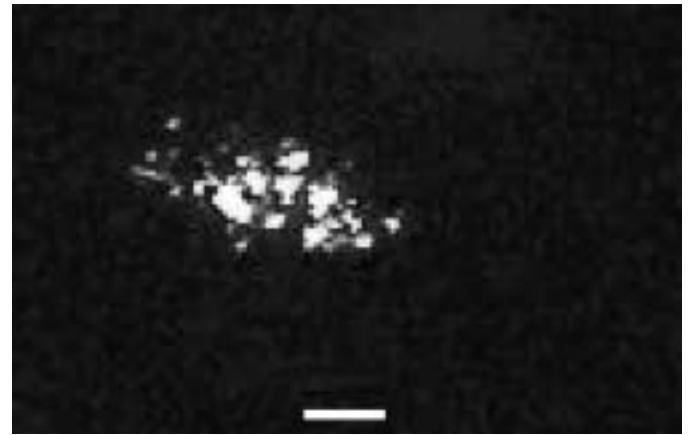


Fig. 4. Microscope image of laser interaction with TFTR sample KC17-2B at 30 W/mm^2 , 50 mm/s, neutral density filter $\times 1000$. The scale bar indicates 1 mm.

viewing area of the pyrometer is an average over these features. It is clear that loosely attached microscopic particles, flakes, and other features strongly modulate the surface thermal conductivity. Features that are poorly thermally connected to the underlying material will experience higher temperature excursions. The range from threshold to saturation of an 8-bit CCD camera signal corresponds to a factor 2–3 temperature change. It is likely that for a pyrometer temperature of $\approx 2000^\circ\text{C}$ some of these particles sublime when the temperature locally reaches the sublimation threshold of 3825°C . In a tokamak this phenomenon could clearly play a significant role in observations of radiation induced sublimation (RES). The surface of JET sample IN3-16 had comparable Be and C concentrations [19] from deposition and preferential erosion of carbon. This is a tokamak generated “mixed material”. After laser exposure, a pattern of $100 \mu\text{m}$ beads appeared on the surface of this sample (Fig. 5).

Some TFTR codeposited samples were imaged in a metallographic microscope (Fig. 6). These specimens were not exposed to the laser and were mounted for grinding and polishing by placing them in 3.2 cm diameter plastic cups. A mixture of epoxy resin and hardener was poured over them, the assembly was pressurized to 35–55 bar with nitrogen and the resin was allowed to solidify overnight. The resin was post-cured at $60\text{--}70^\circ\text{C}$ for two hours to increase its hardness, and the samples were ground on rotating discs coated with fixed diamond abrasive (80, 120, and 220 grit), until the desired amount of material was taken off, typically 1–10 mm. These samples were polished with 30 and 6-micron diamond flat polishing pads with little nap (Struers Pan), a 3 micron diamond Struers Mol pad (wool, low nap),

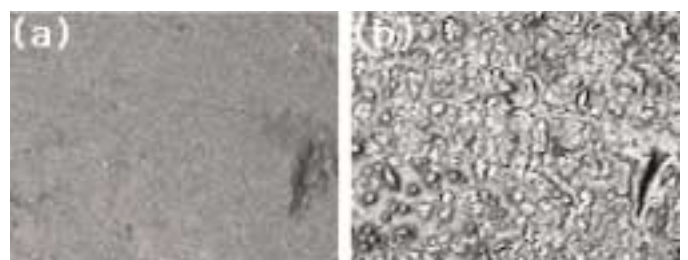


Fig. 5. JET sample IN3-16 with Be/C deposit before (a) and after (b) exposure to laser scans at 2 m/s, 1 m/s and 0.25 m/s at 128 W/mm^2 (see text). Each image covers 2.2 mm in the horizontal direction.

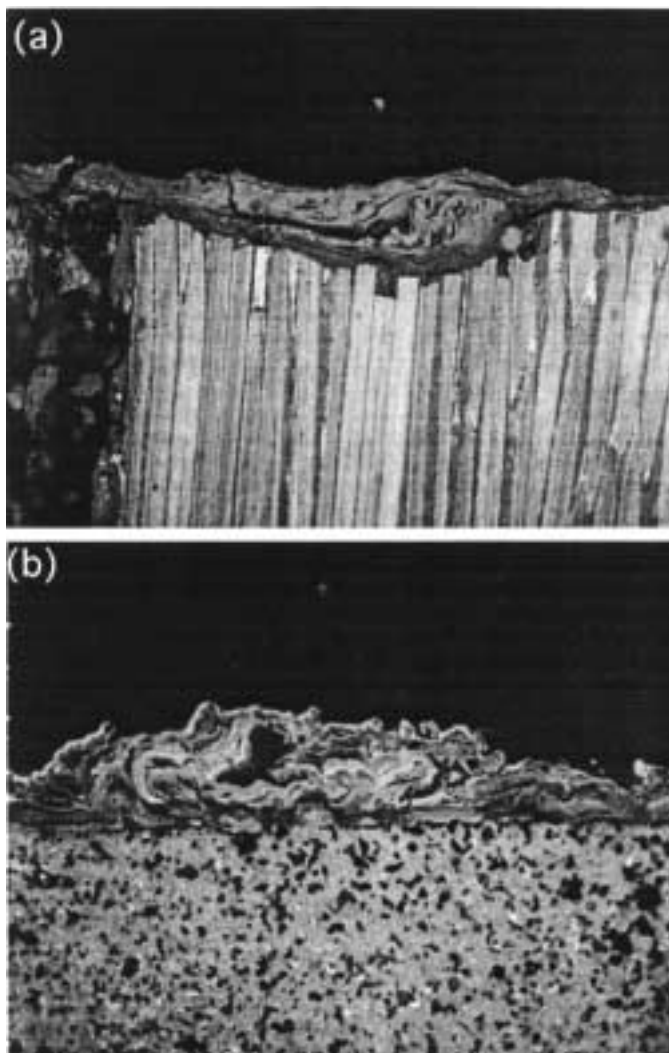


Fig. 6. Microscope images of thick deposits on (a) TFTR carbon-fiber-composite tile KC17-a4.3 surface B-400X, and (b) TFTR graphite tile KC22-V2.3-surface A-400X that have not been exposed to the laser. The images cover 282 microns in the horizontal direction.

and a final polish on 1 micron diamond using Struers Nap cloth—a long nap rayon. Water was the lubricant for all grinding and polishing steps. Microscope images were recorded on Polaroid film, scanned to convert to digital format and the contrast optimized.

The images show a remarkably convoluted structure with distinct strata and voids on multiple spatial scales that is completely different to the manufactured graphite and CFC. The structure reflects the complex history of the last years of plasma operations on TFTR. Earlier images of TFTR codeposits also showed complex structures [20]. Heat transport will be strongly influenced by the complex microstructure of the codeposits. The void spaces will significantly reduce the effective thermal conductivity, and appear to be responsible for the higher surface temperature observed.

5. Summary

Laser scanning offers a convenient way to simulate the effect of high heat flux on codeposited tile samples and to study the effects on important microscopic scales. The high duty cycles planned for next-step tokamaks will inevitably

increase the amount of erosion and deposition by plasma wall interactions. When carbon is used as a plasma facing material the surface of some plasma facing components will be covered by amorphous hydrocarbon deposits with thermomechanical properties significantly different to the manufactured material. The more open porous structure of a codeposit leads to a reduced thermal conductivity and higher surface temperatures with increased duration in response to a transient heat pulse. Microscopic features on the deposit cause spatial variations in conductivity and temperature on a 100-micron scale. Calculations of the thermal response based on the coefficients for manufactured materials will be unrealistic for such deposits. A codeposited plasma facing surface may sublime and generate an impurity influx under high heat flux even though the temperature excursion calculated for the manufactured tile material remains much below the sublimation threshold. Mixed Be/C deposits show “beading” under high heat flux. Reliable predictions for the response of deposition areas to off-normal events such as ELMs and disruptions need to be based on experiments with tokamak generated codeposits.

Acknowledgements

This work is partially funded under the European Fusion Development Agreement, by the UK Department of Trade and Industry, and by U.S. DOE Contract Nos. DE-AC02-76CH0307, and W-31-109-Eng-38.

References

1. Federici, G. *et al.*, Nucl. Fusion **41**, 1967 (2001).
2. Hassanein, A. and Konkashbaev, I., J. Nucl. Mater. **290–293**, 1074 (2001).
3. Wurz, H., Pestchanyi, S., Bazylev, B., Landman, I. and Kappler, F., J. Nucl. Mater. **290–293**, 1138 (2001).
4. Clement, S. *et al.*, J. Nucl. Mater. **266–269**, 285 (1999).
5. Linke, J. *et al.*, “Fusion Technol.” (B. Keen, M. Huguet, and R. Hemsworth, eds.) (1990) pp. 428–423.
6. van der Laan, J. G. *et al.*, J. Nucl. Mater. **196–198**, 612 (1992).
7. Huber, A. *et al.*, Physica Scripta **T94**, 102 (2001).
8. Burtseva, T., Hassanein, A., Ovchinnikov, I. and Titov, V., J. Nucl. Mater. **290–293**, 1059 (2001).
9. Burdakov, A. V. *et al.*, J. Nucl. Mater. **233–237**, 697 (1996).
10. Hassanein, A. and Konkashbaev, I. J. Nucl. Mater. **273**, 326 (1999).
11. Guseva, M. I. *et al.*, J. Nucl. Mater. **220–222**, 957 (1995).
12. Skinner, C. H. *et al.*, J. Nucl. Mater. **301**, 98 (2002).
13. Skinner, C. H., Bekris, N., Coad, J. P., Gentile, C. A. and Glugla, M., Proc. Fifteenth Int. Conf. Plasma-Surface Interactions in Controlled Fusion Devices, Gifu, Japan, May 27–31, to be published in J. Nucl. Mater. (2003).
14. Skinner, C. H. and Federici, G., “Tritium Issues in Next-step Devices”, in “Advanced Diagnostics for Magnetic and Inertial Fusion”, (P. Stott *et al.*, eds.) (Kluwer Academic/Plenum, New York p. 277, 2002).
15. Skinner, C. H. *et al.*, Fusion Sci. Technol. **41**, 716 (2002).
16. Federici, G. *et al.*, Proc. Fifteenth Int. Conf. Plasma-Surface Interactions in Controlled Fusion Devices, Gifu, Japan, May 27–31, to be published in J. Nucl. Mater. (2003).
17. Skinner, C. H., Gentile, C. A. and Hassanein, A., Proc. 19th IEEE/NPSS Symposium on Fusion Engineering (SOFE) Atlantic City, N.J., Jan. 22–25, (2002). IEEE, Piscataway, NJ, USA (2002).
18. Paffett, M. T., Willms, R. S., Gentile, C. A. and Skinner, C. H., Fusion Sci. Technol. **41**, 934 (2002).
19. Coad, J. P. *et al.*, J. Nucl. Mater. **290–293**, 224 (2001).
20. Mills, B. E., Buchenauer, D. A., Pontau, A. E. and Ulrickson, M., J. Nucl. Mater. **162–164**, 343 (1989).